Colloids and Surfaces B: Biointerfaces 220 (2022) 112867

Contents lists available at ScienceDirect

Colloids and Surfaces B: Biointerfaces

journal homepage: www.elsevier.com/locate/colsurfb

Structure and activity of native and thiolated α-chymotrypsin adsorbed onto gold nanoparticles

McKenzie B. Riley [1], Evan Strandquist, Christopher S. Weitzel [2], Jeremy D. Driskell [*,3]

Department of Chemistry, Illinois State University, Normal, IL 61790, United States

ARTICLE INFO

Keywords:
Gold nanoparticle
Bioconjugate
α-chymotrypsin
Protein adsorption

ABSTRACT

A detailed understanding of protein-nanoparticle interactions is critical to realize the full potential of bioconjugate-enabled technologies. Parameters that lead to conformational changes in protein structure upon adsorption must be identified and controlled to mitigate loss of biological function. We hypothesized that the installation of thiol functional groups on a protein will facilitate robust adsorption to gold nanoparticles (AuNPs) and prevent protein unfolding to achieve thermodynamic stability. Here we investigated the adsorption behavior of α-chymotrypsin (ChT) and a thiolated analog of α-chymotrypsin (T-ChT) with AuNPs. ChT, which does not present any free thiols, was modified with 2-iminothiolane (Traut's reagent) to synthesize T-ChT consisting of two free thiols. Protein adsorption to AuNPs was monitored with dynamic light scattering and UV–vis spectrophotometry, and fluorescence spectra were acquired to assess changes in protein structure induced by interaction with the AuNP. The biological function of ChT, T-ChT, and respective bioconjugates were compared using a colorimetric enzymatic assay. The thiolated analog exhibited a greater affinity for the AuNP than the unmodified ChT, as determined from adsorption isotherms. The ChT protein formed a soft protein corona in which the enzyme denatures with prolonged exposure to AuNPs and, subsequently, lost enzymatic function. Conversely, the T-ChT formed a robust hard corona on the AuNP and retained structure and function. These data support the hypothesis, provide further insight into protein-AuNP interactions, and identify a simple chemical approach to synthesize robust and functional conjugates.

1. Introduction

Emerging bionanotechnologies that exploit the synergistic properties of protein-nanoparticle bioconjugates hold great promise for the advancement of many fields, including biosensing [1], imaging [2,3], photothermal therapy [4], drug delivery [5], and biocatalysis [6,7]. A detailed understanding of the protein-nanoparticle interface is critical to mitigate structural changes that negatively impact the function of the adsorbed protein and leverage stabilizing interactions that enhance protein function.

A significant loss of function has been reported for several proteins after adsorption onto nanoparticles, including lysozyme, chymotrypsin, fibrinogen, and RNase A [8–11]. Conversely, the functional properties of other proteins have been preserved or even enhanced upon adsorption to nanoparticle supports [12–16]. Previous efforts have investigated the effect of nanoparticle size [17,18], curvature [19,20], ligand charge [21–23], and protein deformability [24] on protein function; however, a universal predictor of behavior has yet to be elucidated. For example, the structure and function of lysozyme was retained when adsorbed on small nanoparticles, but decreased as the size of the nanoparticle support increased [8], whereas the activity of RNase A decreased as nanoparticle size decreased [11]. The function of the adsorbed protein is system dependent, and currently there is no predictive model that correlates the characteristics of a protein or nanoparticle with gain or loss of function.

A protein may undergo conformational changes upon adsorption to a nanoparticle [25–28]. These adsorption-induced structural changes can expose previously buried domains and lead to further denaturation as the protein unfolds to optimize protein-nanoparticle interactions for thermodynamic stability. Specifically for gold nanoparticles, recent

* Corresponding author.
E-mail address: jdriske@ilstu.edu (J.D. Driskell).
[1] Current address: Biomedical Sciences, University of Alabama at Birmingham.
[2] Current address: Department of Chemistry, Texas A&M University.
[3] orcid.org/0000-0001-5082-898X

https://doi.org/10.1016/j.colsurfb.2022.112867
Received 6 July 2022; Received in revised form 16 September 2022; Accepted 19 September 2022
Available online 22 September 2022

work probing the adsorption of immunoglobulin G, bovine serum albumin, pyrophosphatase, and GB3 suggests that the thermodynamically preferred interaction involves the formation of a Au-S bond between cysteine and the gold nanoparticle [29–35], although adsorption through amines may also contribute [36–38]. Consistent with these works, Fitzkee et al. proposed a three-step process to describe the adsorption of protein to a nanoparticle [33]. According to this model, proteins reversibly associate with the nanoparticle surface, rearrange/reorient on the surface, and harden to form an irreversible protein layer. Thus, if cysteine residues are present on the surface of the protein, denaturation may not be necessary in the second step of the adsorption process for hardening to occur in the third step. Indeed, work on the immobilization of enzymes have found that immobilization may result in a rigidification of the enzyme structure to preserve catalytic activity [39–41]. Moreover, structural integrity can be further preserved through multiple points of attachment [12]. Recent work in our group found that the antigen-binding function of antibody immobilized onto AuNP is dependent on the presence of solvent accessible high affinity moieties on the protein [42]. Thus, it is interesting to consider the accessibility of functional groups presented by the protein that exhibit a high affinity for the AuNP surface and the functional fate of the adsorbed protein.

Here we investigate the effect of surface accessible thiol groups on a protein on the structure and function of the adsorbed protein. α-Chymotrypsin (ChT) is a well-characterized enzyme that was selected as a model protein for this study. ChT is a serine protease enzyme that selectively catalyzes the hydrolysis of peptide bonds on the C-terminal side of tyrosine, phenylalanine, tryptophan, and leucine, and its biocatalytic activity is easily monitored spectrophotometrically. ChT is ideal for this study because the native protein does not contain free thiols. In this work, thiols are installed onto ChT through chemical modification of lysine residues with 2-iminothiolane (Traut's reagent). Subsequently, the adsorption behavior of native ChT and the thiolated ChT (T-ChT) analog onto AuNP are directly compared. Thus, it is possible to elucidate the impact of free thiols on protein adsorption by ensuring that other parameters previously reported to influence protein-NP binding are equivalent for both protein-NP systems, e.g., molecular weight, protein charge, and amino acid sequence.

2. Experimental

2.1. Materials and reagents

AuNPs were obtained from Ted Pella (Redding, CA) with a diameter of 60 nm at a concentration of 2.6×10^{10} (particles/mL). Potassium phosphate monobasic was obtained from Thermo Scientific (Rockford, IL) and potassium phosphate dibasic is from Mallinckrodt Chemical (St. Louis, MO). Traut's reagent, Ellman's reagent, and lyophilized horseradish peroxidase (HRP) were purchased from Thermo Scientific. In all studies, type II α-chymotrypsin from bovine pancreas in a lyophilized powder from Sigma Aldrich (St. Louis, MO) was used. Monoclonal anti-horseradish peroxidase (anti-HRP) antibody isolated from a mouse was obtained from MyBioSource (San Diego, CA). All chemicals were used as received without further purification.

2.2. Protein modification with Traut's reagent

For modification of solvent-exposed lysine residues on ChT, freshly prepared 2-iminothiolane (Traut's Reagent, 20 μL, 50 mM) was added to ChT (500 μL, 2 mg/mL) and incubated for 1 h at room temperature with gentle shaking. After incubation, the modified protein (T-ChT) was purified using a desalting column. Following the manufacturer's protocol, the column was centrifuged at 1500 g for 1 min to remove the initial storage solution. To charge the column, 300 μL of phosphate buffer (2 mM, pH 8.0) was added and centrifuged at 1500 g for 1 min. This was repeated three times, with the buffer being discarded after each wash. In a new centrifuge tube, 300 μL of T-ChT was added to the column with a 15 μL stacker buffer (2 mM phosphate buffer, pH 8.0). The column was centrifuged at 1500 g for 2 min and the final solution was collected. The final concentration of T-ChT was determined through UV–visible spectroscopy and calculated with an extinction coefficient ($E^{1\%}$) of 20.4 at 280 nm [43].

2.3. Determination of free thiols with Ellman's reagent

5,5-dithio-bis-(2-nitrobenzoic acid) (Ellman's reagent, 4 mg) was dissolved in 1 mL of phosphate buffer (0.1 M, pH 8.0) containing 0.1% EDTA. Cysteine standards at concentrations of 0.1–1.0 μM were prepared. In a clear 96-well plate, 46.5 μL of 2 mM phosphate buffer and 3.5 μL of freshly prepared Ellman's reagent were added to each well and 10 μL of standard/sample were then added. The mixture was allowed to react for 30 min at room temperature and the absorbance was obtained at 415 nm.

2.4. Sodium dodecyl sulfate-polyacrylamide gel electrophoresis (SDS-PAGE)

Non-reducing SDS-PAGE conditions were employed for analysis of ChT and T-ChT. Briefly, enzyme at a concentration of 50 μg/mL was prepared. Samples were diluted in loading buffer (75 mM Tris-HCl, 20 % (v/v) glycerol, 0.1 % (w/v) bromophenol blue, 2 % (w/v) SDS, pH 8.30) and heated at 75 °C for 10 min with occasional vortexing. Heated samples were centrifuged and loaded (10 μL) on a standard Laemmli 8 % tris-glycine SDS gel alongside BioRad Precision Plus protein standard. The gel was run in 1x tris-glycine running buffer (25 mM tris base, 192 mM glycine, 0.1 % (w/v) SDS, pH 8.30) at 120 V for 60 min followed by silver staining using the Pierce® Silver Stain for Mass Spectrometry kit as per the manufacturer's recommended protocol.

2.5. Conjugation of proteins to AuNPs

Protein immobilization onto AuNPs was completed as previously described [44–46]. Briefly, AuNPs (60 nm, 100 μL) were added to a low-binding centrifuge tube, and phosphate buffer (4 μL, 50 mM) was added to adjust the pH of the suspension to 8.0. The protein sample, ChT or T-ChT, was added to the AuNP suspension and incubated for 1 h at room temperature, unless noted otherwise. After incubation, the functionalized AuNPs were centrifuged at 5000 g for 5 min, the supernatant was removed, and the pelleted AuNPs were resuspended in phosphate buffer (2 mM, pH 8.0). The functionalized AuNPs were subsequently washed and pelleted three more times to thoroughly remove excess protein.

2.6. Salt induced aggregation kinetics

The stability of the formed protein corona was tested with salt-induced aggregation. Sodium chloride (100 mM final concentration) was introduced into the functionalized AuNP solution and thoroughly mixed prior to beginning UV–vis kinetics measurements. A wavelength scan from 400 to 900 nm with 0.50 nm increments was obtained once every min for 20 min, and the ratio of $A_{800\ nm}$ to $A_{538\ nm}$ was calculated at each time point to quantitatively assess the rate of aggregation [47].

2.7. Enzyme activity assay

The enzymatic activity of ChT and its analog was determined using N-benzoyl-L-tyrosine *p*-nitroanilide (BTNA) as the substrate [48]. ChT catalyzes the cleavage of BTNA to produce p-nitroaniline which exhibits strong absorption at 380 nm. To measure the enzymatic activity, 180 μL of sample were mixed with 20 μL of 1 mM BTNA in a clear 96-well plate. BTNA was dissolved in a DMSO/ethanol (1:9) mixture. The absorbance at 380 nm was monitored at 1-min intervals for 20 min to measure the

formation of the *p*-nitroaniline product, and the enzymatic activity was defined as the average reaction rate.

2.8. Protein exchange on protein-AuNP bioconjugate

ChT-AuNP and T-ChT-AuNP conjugates were prepared as described above. The adsorbed ChT and T-ChT were displaced from the AuNP surface by the introduction of a competing protein, anti-HRP antibody, that has been previously established to possess a high affinity for AuNPs [44,45]. Briefly, 3 μg of anti-HRP antibody was added to 100 μL of purified ChT-AuNP and T-ChT-AuNP conjugates and incubated for 3 h to allow for protein exchange on the AuNP surface. Next, the conjugates were centrifuged at 5000 g for 5 min and the supernatant was collected for further analysis. The supernatant was first passed through a Vivacon 500 filtration device (2 kDa MWCO) to concentrate the proteins. Briefly, filters were pre-washed twice with 500 μL phosphate buffer (2 mM, pH 8.0) and centrifuged at 14,000 g for 15 min. Next, 200 μL of sample and 300 μL of buffer were added to the filters and centrifuged at 14,000 g for 30 min. The filtration device was then inverted into a new centrifuge tube and centrifuged at 2500 g for 2 min to collect the concentrated protein. The concentrated supernatant, ChT and T-ChT controls, and method controls (e.g., antibody and ChT or T-ChT mixtures passed through Vivacon 500 filter) were then electrophoresed via SDS-PAGE using reducing conditions (e.g., loading buffer included 0.75 % (v/v) β-mercaptoethanol) to confirm the displacement of the ChT and/or T-ChT from the AuNP surface. Additionally, the concentrated supernatant was evaluated for enzyme activity using BTNA to determine the activity of the enzyme displaced from the AuNP surface. The pelleted AuNP conjugate was resuspended in 2 mM phosphate buffer (pH 8.0) and the centrifugation/resuspension cycle was repeated twice more to purify the antibody-AuNP conjugates formed by protein exchange. An antigen capture assay was performed to confirm the formation of the antibody-AuNP conjugate (Supporting Information).

2.9. Solvent accessibility of amino acids

The SABLE Server was used to predict the relative solvent accessibility of amino acid residues in α-chymotrypsin. Using the amino acid sequence for α-chymotrypsin (PDB 4CHA), SABLE outputs a value ranging from 0 to 1 for each amino acid residue to represent the relative solvent accessibility. A residue that is completely inaccessible is given a value of 0, whereas a residue that is fully exposed is given a value of 1 [49–51].

2.10. Instrumentation

Characterization of conjugates was carried out on a Malvern Zetasizer Nano ZSP from Malvern Panalytical (Westborough, MA) for dynamic light scattering (DLS) measurements. UV–visible measurements were obtained on a Cary 3500 UV–visible spectrophotometer from Agilent (Santa Clara, CA) operating from 400 to 800 nm with a spectral bandwidth of 0.5 nm. Fluorescence measurements were obtained from a Cary Eclipse fluorescence spectrophotometer from Agilent scanning from 320 to 380 nm. All well plate absorbance measurements were accomplished with a Varioskan LUX multimode microplate reader from Thermo Scientific.

3. Results and discussion

3.1. Modification and characterization of α-chymotrypsin

The structure of α-chymotrypsin (ChT) is presented in Fig. 1 [52]. The structure reveals 20 cysteine residues in which all are involved in disulfide bonds. Free thiols were installed onto ChT by reacting with Traut's reagent to create a thiolated ChT analog (T-ChT) and to study the impact of thiols on the structure and function of the enzyme upon adsorption to citrate-capped gold nanoparticles with a nominal diameter of 60 nm. Specifically, Traut's reagent was selected as the chemical modifier because it reacts with primary amines available on lysine residues and installs a free thiol functional group (Fig. S1).

Chemical modification of ChT was confirmed by use of Ellman's reagent and a cysteine calibration curve to quantify the number of free thiols on native ChT and the synthesized T-ChT (Fig. S2) [54]. No free thiols were detected on ChT, confirming that cysteine residues are involved in disulfide bridges, as determined by crystallography (Fig. 1A). T-ChT was synthesized with a 25-fold molar excess of Traut's reagent to modify all reactive amines. Analysis of T-ChT found that 2.0 ± 0.7 free thiol groups were installed on each T-ChT molecule and establishes successful modification with Traut's reagent. The reaction of Traut's reagent with a lysine residue requires that the amino group on the side chain is deprotonated and solvent accessible. Examination of the electrostatic potential map (Fig. 1B) and relative solvent accessibility (Fig. 1C) suggests that Lys84 and Lys93 are most likely to be modified based on accessibility and favorable charge, e.g., neutral to slight positive charge. Lys170 is highly accessible, but likely not reactive due to its protonation state. Lysines at positions 36, 79, 202, and 203 are predicted to exhibit favorable charge states with moderate accessibility; thus, while less probable, these are also potential sites for modification. Collectively, these data support the experimentally measured number of installed thiols.

Protein modification can lead to unwanted protein denaturation and/or aggregation through intermolecular disulfide bridging; therefore, native ChT and chemically modified T-ChT were analyzed using SDS-PAGE under non-reducing conditions to evaluate the impact of

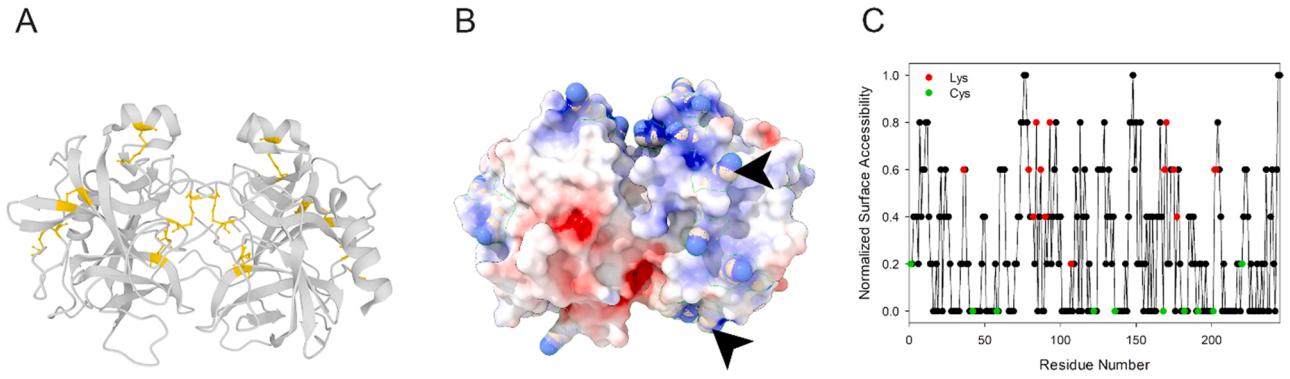

Fig. 1. (A) Structure of α-chymotrypsin (PDB 4CHA). Cysteine residues are highlighted in yellow and each is a participant in a disulfide bond [52]. (B) Electrostatic potential surface map of α-chymotrypsin calculated at pH 8.0. Lysine residues are overlaid as spheres and Lys84 and Lys93 are marked with black arrows. The blue represents positive potential, and the red represents negative potential, with a range from − 5 k_bT/e to + 5 k_bT/e [53]. (C) Relative solvent accessibility of each amino acid in α-chymotrypsin with lysine residues shown as red data points and cysteine highlighted as green data points.

chemical modification on the protein oligomerization state. Importantly, equivalent mobilities are observed for ChT and T-ChT suggesting the chemical modification did not render the protein unstable (Fig. 2A). However, it is noted that the globular, non-reduced ChT and T-ChT samples migrated with reduced mobility as compared to the linearized protein of similar molecular weight (~ 25 kDa) within the ladder. This is expected as intramolecular disulfide bonds have been shown to reduce the mobility of a protein [55–59]. ChT and T-ChT were further characterized with respect to enzymatic reaction rate to evaluate if the thiolation of two lysine residues influenced the biological activity of ChT. To this end, solutions of ChT and T-ChT were each prepared at 27.5 μg/mL and reacted with BTNA, a substrate previously employed to assess enzymatic activity of ChT [48]. ChT catalyzes the hydrolysis of the BTNA amide bond to produce p-nitroaniline which enables the reaction rate to be measured spectrophotometrically. Equivalent reaction rates were observed for ChT and T-ChT (Fig. 2B) and establish that the installation of thiol functional groups on ChT to form T-ChT does not significantly alter the enzyme structure/function.

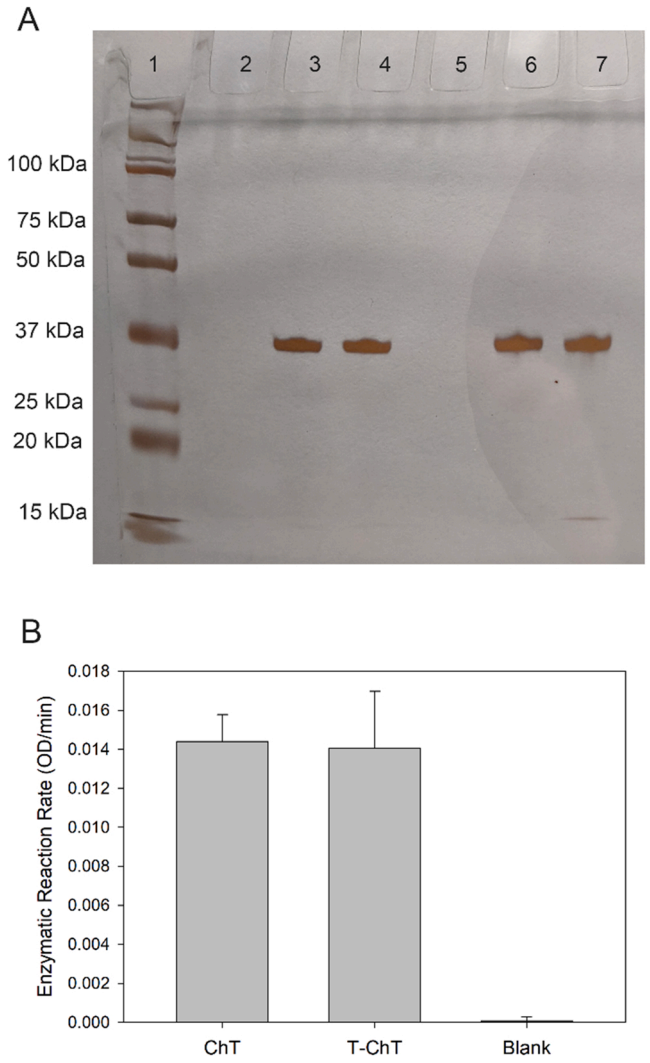

Fig. 2. (A) Image of non-reducing gel for SDS-PAGE analysis of ChT (lanes 3 and 4) and T-ChT (lanes 6 and 7). Each sample was prepared in duplicate. (B) Enzymatic rates of unmodified ChT (ChT) and after modification with Traut's reagent (T-ChT). Each enzyme sample was prepared at 27.5 μg/mL. Incubation of the BTNA substrate with phosphate buffer (2 mM, pH 8.0) in the absence of enzyme served as the negative control (Blank).

3.2. Adsorption of ChT and T-ChT onto gold nanoparticles

Adsorption isotherms were generated to compare the interaction between ChT or T-ChT and AuNPs. Varying concentrations of protein (0–60 μg/mL) were introduced to a suspension of AuNPs and allowed to incubate for 1 h. Dynamic light scattering (DLS) was used to measure the hydrodynamic diameter of the protein-AuNP conjugate as a means to monitor adsorption. Fig. 3 establishes that both ChT and T-ChT spontaneously adsorb onto AuNPs, saturate at monolayer coverage, and form stable bioconjugates. The thickness of the protein layer at monolayer coverage and the adsorption affinity (K_d) were extracted from a best fit of the adsorption isotherms to the Langmuir model (Fig. 3). The greater binding affinity exhibited by T-ChT is anticipated based on the installation of free thiols that are known to strongly interact with gold surfaces [31,44]. Additionally, the T-ChT layer is slightly thicker than the ChT layer on the AuNP and implies differences between ChT and T-ChT with respect to protein orientation, loading, or structure (denatured/deformed) when adsorbed onto the AuNP.

The protein-AuNP conjugates were then centrifuged to remove loosely bound proteins from the AuNP surface and again analyzed with DLS to distinguish between the hard and soft protein corona [60–63]. Fig. 4A shows a marked decrease in D_H after centrifuging the ChT-AuNP conjugates and removing excess/weakly bound ChT molecules for each ChT concentration. This data suggests a significant fraction of the ChT molecules were loosely adsorbed onto the AuNP. The fully saturated conjugates maintained an ~4 nm increase in D_H relative to the unconjugated AuNP confirming another fraction of the ChT molecules formed a hard corona. In contrast, centrifugation of the T-ChT-AuNP conjugates resulted in an insignificant decrease in the D_H of the conjugates (Fig. 4B). These data establish the T-ChT-AuNP interaction is robust, and the protein corona can be characterized as primarily hard. Extinction spectra corroborate the DLS data and support the protein corona description (Fig. 4C and D). The surface plasmon resonance (SPR) band for the ChT conjugate red shifted from 535 nm for the unconjugated AuNP to 539 nm after ChT adsorption, prior to centrifugation, e.g., combined hard and soft protein corona. This 4-nm shift in SPR resulted from a change in the local refractive index at the AuNP surface upon protein adsorption and is consistent with previously reported values for protein adsorption [64,65]. After centrifugation, the SPR band was centered at 536 nm and confirms the partial removal of adsorbed ChT, e.g., loosely associated ChT molecules. In comparison, the SPR band of the

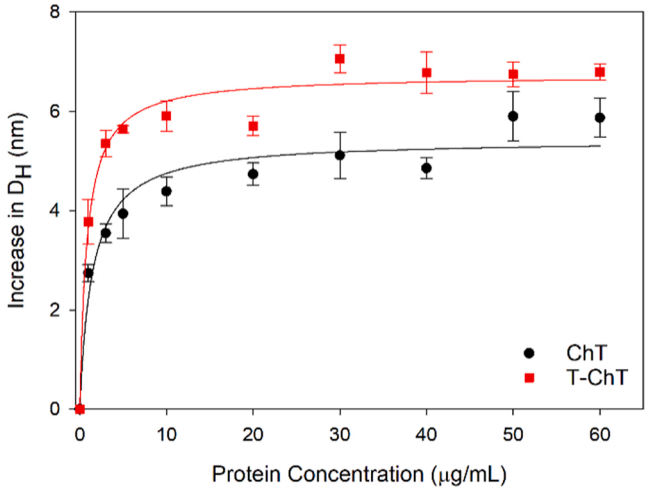

Fig. 3. Adsorption isotherms generated by plotting the increase in hydrodynamic diameter (ΔD_H) of the conjugate relative to the unconjugated AuNP for the adsorption of ChT (black circles) and T-ChT (red squares) at 1.0–60 μg/mL. The data were best fit to the Langmuir adsorption isotherm model (solid lines). ChT resulted in $\Delta D_{H,max}$ of 5.43 ± 0.22 nm and K_d of 1.43 ± 0.38 μg/mL; T-ChT resulted in $\Delta D_{H,max}$ of 6.73 ± 0.17 nm and K_d of 0.84 ± 0.17 μg/mL.

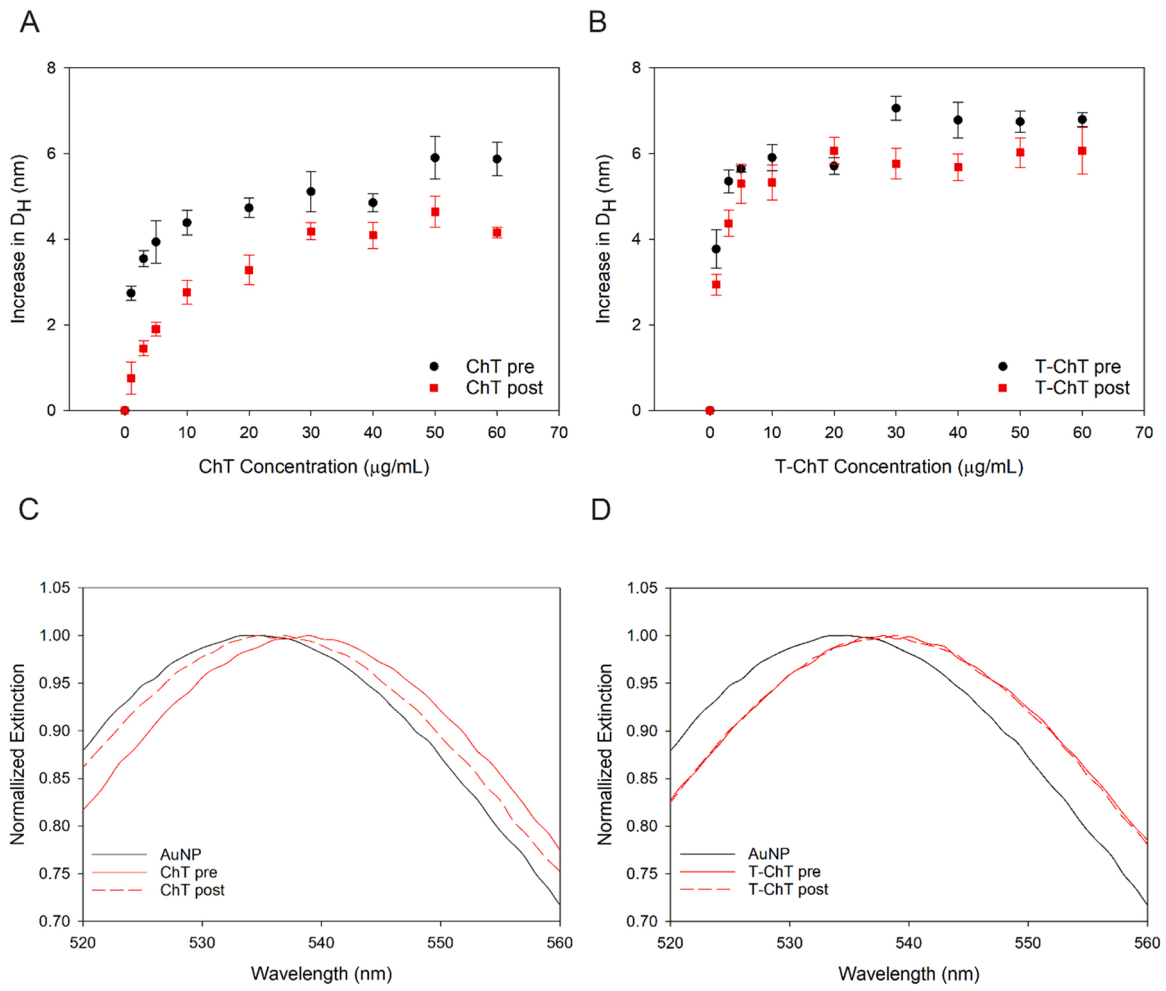

Fig. 4. Adsorption isotherms of ChT (A) and T-ChT (B) for 1.0–60 μg/mL of protein after conjugation to AuNP. DLS data was obtained after conjugation pre (black) and post (red) purification via centrifugation. Representative UV-Vis spectra of ChT (C) and T-ChT (D) conjugates (30 μg/mL). Black line indicates unconjugated AuNP. Solid (red) and dashed (red) lines indicate pre and post purification of conjugates, respectively.

T-ChT-AuNP was located at 539 nm both before and after centrifugation, confirming the associated T-ChT layer on the AuNP surface remained intact.

The overall stability of the protein-AuNP conjugates was investigated with salt induced aggregation kinetics. The presence of a hardened protein corona protects AuNPs from aggregation as electrolytes are introduced to cause a collapse of the electrical double layer [66,67]. After bioconjugate purification, NaCl was added to ChT-AuNP and T-ChT-AuNP conjugates and extinction spectra were acquired as a function of time to monitor aggregation (Figs. S3A and S3B). As is

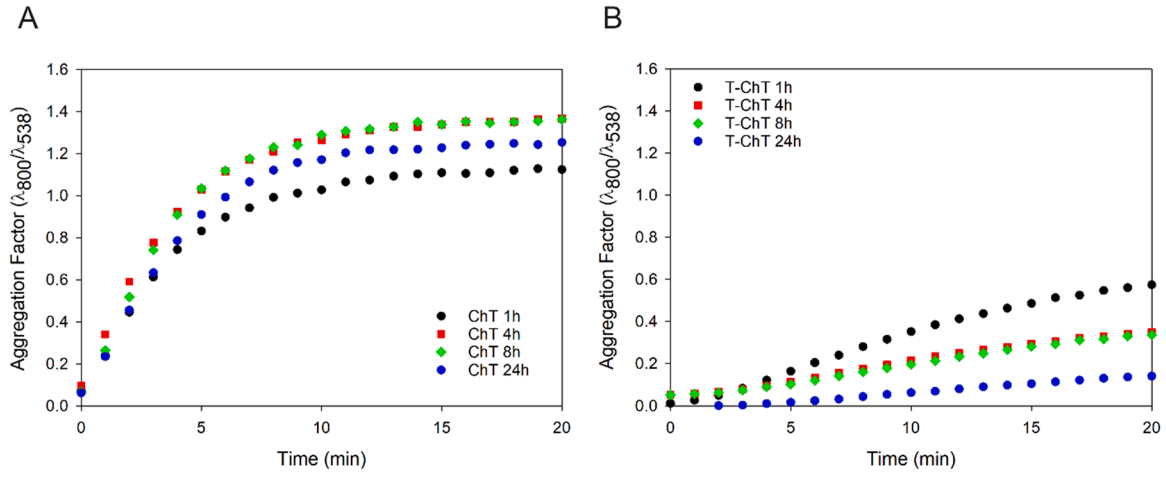

Fig. 5. Aggregation factors as a function of time in a saline environment for ChT-AuNP conjugates (A) and T-ChT-AuNP conjugates (B), where the enzyme was allowed to adsorb onto the AuNP for 1 h (black), 4 h (red), 8 h (green), and 24 h (blue) prior to the addition of salt.

evident in Figs. S3A and S3B, the magnitudes of the SPR band ($\lambda_{538\ nm}$) decreases and the aggregation band ($\lambda_{800\ nm}$) increases at a faster rate for ChT-AuNP conjugate than the T-ChT-AuNP conjugate. Aggregation was quantified by calculating the aggregation factor (AF) at each time point, where AF is defined as the ratio of the extinction of the emerging aggregation peak at 800 nm and extinction of the SPR peak position at 538 nm (Eq. 1) [47].

$$AF = \frac{A_{800}}{A_{538}} \quad (1)$$

Fig. 5A and B establish that the thiolated T-ChT forms a more stable conjugate than the unmodified ChT and is consistent with the DLS and extinction spectra demonstrating that T-ChT forms a hard corona on the AuNP, while ChT molecules form a mixed soft/hard corona.

Previous works have found that the protein corona is dynamic and that loosely bound proteins in the soft corona can reorient/unfold with increased incubation time to increase the binding affinity and harden [33,42]. To explore this time-dependent corona formation, ChT and T-ChT were incubated with AuNP for varying amounts of time (1 – 24 h) to allow for protein adsorption. Subsequently, the conjugates were centrifuged to remove the soft protein corona and then subjected to NaCl treatment and monitored via extinction spectroscopy to evaluate the conjugate stability. Fig. 5A shows similar aggregation kinetics independent of the time allowed for ChT to adsorb, suggesting that no additional corona hardening occurred beyond 1 h of interaction. However, increased incubation time allowed T-ChT to form a more stable conjugate, likely by reorientation of molecules to position the installed thiol moiety adjacent to the AuNP surface for chemisorption (Fig. 5B).

The concentration of protein adsorbed on the AuNP was determined using an indirect method in which a defined concentration of protein is added to the conjugate and the excess unbound is quantified. Protein loading is calculated as the difference in the concentration of protein added to the AuNP and the concentration of protein that remains in the supernatant. Initially, we attempted to use native protein fluorescence to quantify protein in the supernatant [68]; however, we observed a difference in the emission spectra for the unbound ChT relative to standard solutions of ChT, suggesting inherent structural differences between the two. Consequently, accurate calibration and comparison of ChT and T-ChT concentrations were not possible based on protein fluorescence. Subsequently, a bicinchoninic acid (BCA) total protein assay was used to accurately quantify the unbound protein (Fig. S4). Guided by adsorption isotherms presented in Fig. 3, a total of 15 μg of ChT or T-ChT were added to 1.0 mL of AuNP and allowed to incubate for 1 h to saturate the AuNP surface at maximum coverage. The formed protein-AuNP conjugate was harvested via centrifugation, and the protein in the remaining supernatant was quantified using a BCA microassay with ChT and T-ChT solutions as calibration standards. Based on the protein added and that remaining in the supernatant, 4.51 and 7.75 μg/mL of ChT and T-ChT,

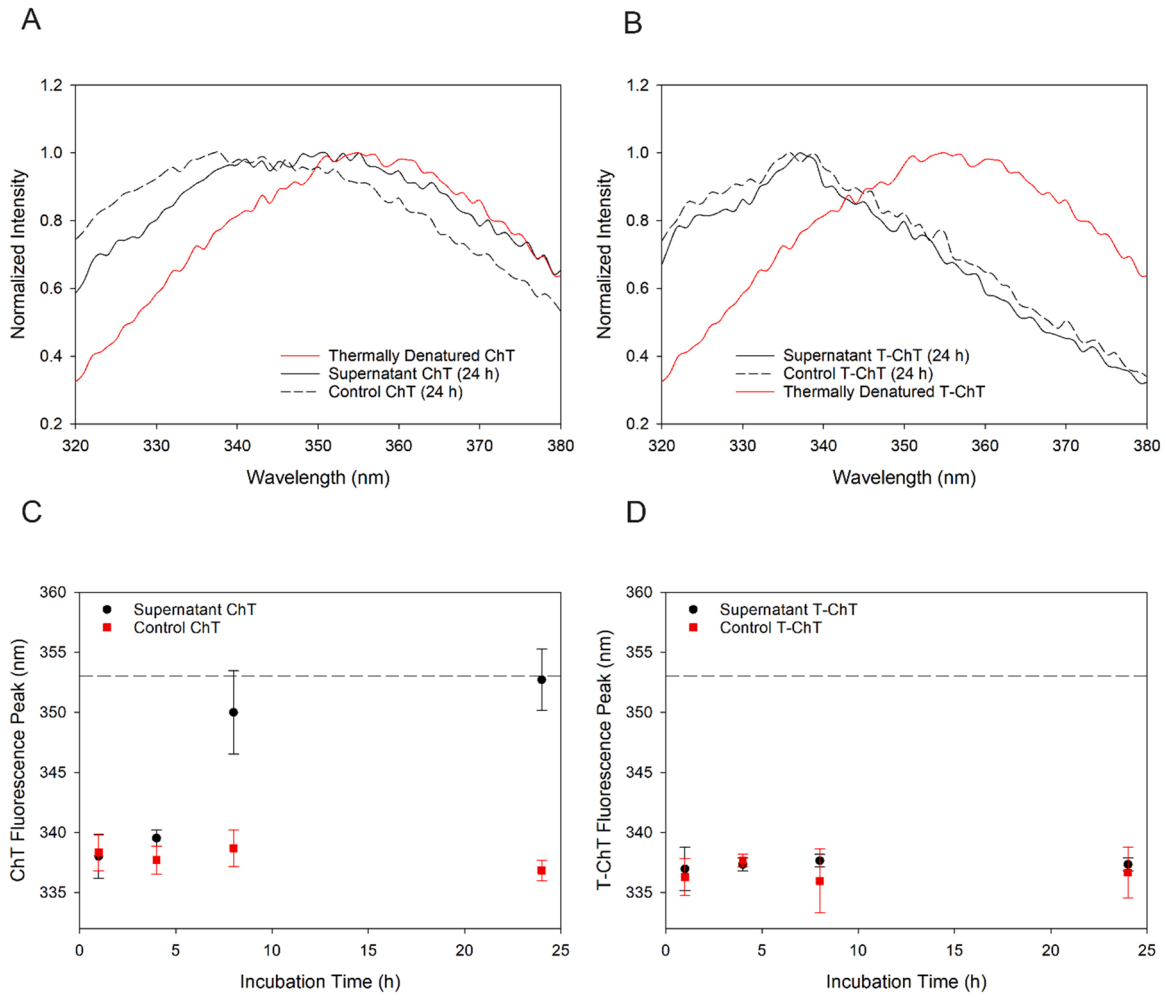

Fig. 6. Normalized fluorescence spectra for ChT (A) and T-ChT-AuNP (B) collected as the supernatant after incubation with AuNPs for 24 h (solid black line). ChT and T-ChT prepared and stored at room temperature for 24 h prior to analysis were analyzed as negative control samples. ChT and T-ChT were thermally denatured and analyzed to serve as positive control samples. Plotted fluorescence peak position of ChT (C) and T-ChT (D) where black and red are supernatant samples and controls, respectively. The horizontal dashed line marks the peak position for the thermally denatured positive control samples.

respectively, were adsorbed onto the AuNP. These measured values are consistent with the DLS data and extinction spectra determining the hard and soft corona, as well as the kinetics of the salt-induce aggregation.

As noted above, differences in fluorescence emission spectra were observed for excess, unbound ChT separated from the formed AuNP conjugate. It is widely established that the intrinsic fluorescence of tryptophan residues is very sensitive to protein conformational changes and can provide valuable information about changes in the secondary and tertiary structure [69,70]. Thus, additional fluorescence studies were conducted to gain insight into structural changes induced by exposure to AuNPs. The fluorescence spectrum of a freshly prepared solution of ChT and excess ChT collected in the supernatant after 24 h of incubation with AuNP are presented in Fig. 6A. A significant bathochromatic shift in the fluorescence maximum is noted for the ChT after incubation with the AuNP. Fig. 6B shows that the fluorescence spectra of freshly prepared T-ChT and T-ChT collected in the supernatant after 24 h of incubation with AuNP are equivalent to that of freshly prepared ChT, i.e., no spectral shift. Thus, this data suggests that ChT adsorbs onto AuNP, undergoes significant changes in secondary structure, and then desorbs from the AuNP surface. Conversely, the T-ChT adsorbs onto the AuNP to remain bound and prevents the excess T-ChT in the supernatant from interacting with the AuNP surface. Therefore, the secondary structure of the T-ChT in the supernatant is not altered; however, no insight into the structure of the immobilized T-ChT is obtained. Fluorescence spectra were also collected for thermally denatured proteins and confirmed the red shift can be attributed to protein denaturation (Fig. 6A and B). Time-dependent fluorescence spectra were then collected to determine if there is a correlation between incubation time with the AuNP and increased changes in protein secondary structure (Fig. 6C and D). A significant shift in the fluorescence maxima is noted for the ChT-AuNP samples after the 8 h incubation period, with peak positions close to the thermally denatured control sample. We note the fluorescence spectrum is an average of the protein population and we deduce that no shifts are observed for ChT after 1 h and 4 h of incubation with AuNP because the fluorescence spectrum is dominated by a large excess of ChT molecules that has not had sufficient time to interact with the AuNP. In comparison, no such shift is noted for the T-ChT-AuNP conjugates at all time points.

3.3. Activity of bioconjugates

The enzymatic activity of the purified enzyme-AuNP conjugates was analyzed. To this end, ChT-AuNP and T-ChT-AuNP conjugates were prepared, and excess, unbound enzyme was removed from the conjugate suspension. BTNA was mixed with the isolated conjugate and the absorbance of the product was monitored at 380 nm to assess the enzymatic activity. A negative control sample was prepared as the addition of BTNA to buffer, in the absence of enzyme. The reaction rates for both the ChT-AuNP and T-ChT-AuNP conjugates were statistically equivalent to that of the negative control (Fig. 7); thus, we concluded that neither conjugate was enzymatically active. It should be noted that ChT-AuNP conjugates were previously reported to be catalytically active towards BTNA [48]. However, in that work it was assumed that ChT was exhaustively adsorbed onto the AuNP, thus, not requiring a purification step to isolate the ChT-AuNP conjugates from excess ChT.

Enzymatic activity can provide valuable insight into the orientation or structural changes of the adsorbed enzyme. A loss in activity, as observed in this system, could suggest that the active site is inaccessible due to the orientation of the enzyme or that the interaction with the AuNP surface induces structural changes, i.e., unfolding, that have functional consequences. To identify which of these two factors causes the decrease in enzyme activity, the adsorbed enzyme was displaced from the AuNP surface, and the enzyme recovered in solution was evaluated for enzymatic activity. This was achieved using an approach recently reported by our lab, in which an IgG antibody was added to the

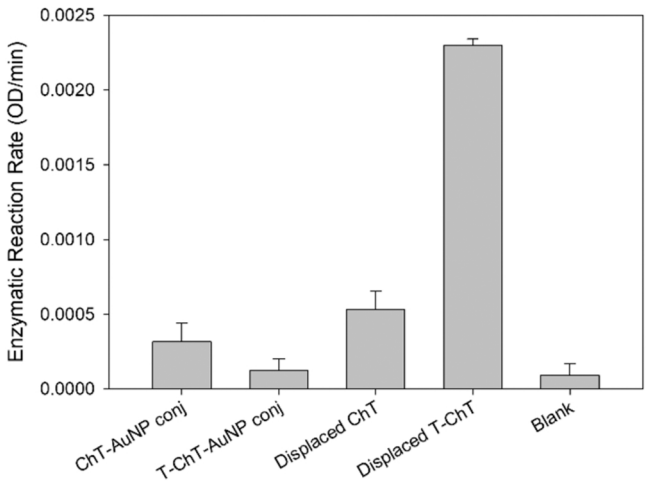

Fig. 7. Enzymatic rates of ChT and T-ChT adsorbed onto AuNP (conjugates) and enzymatic rates of ChT and T-ChT displaced from the surface of the AuNP by an IgG protein. Incubation of the BTNA substrate with phosphate buffer (2 mM, pH 8.0) in the absence of enzyme served as the negative control (Blank).

enzyme-AuNP conjugate to displace the pre-adsorbed ChT or T-ChT on the AuNP surface [44]. To confirm protein exchange on the AuNP surface was successful, the conjugates were centrifuged and the unbound proteins present in the supernatant were analyzed via reducing SDS-PAGE. In Fig. 8, a band with an approximate molecular weight of 15 kDa is observed for the ChT (lane 9) and T-ChT (lane 10) displaced from the AuNP surface. These bands are consistent with the molecular weight of the ChT B chain that is observed in the control lanes containing freshly prepared ChT (lane 3) and T-ChT (lane 4), as well as concentrated ChT (lane 5) and T-ChT (lane 6). Importantly, this protein band is absent in the antibody control sample (lane 2) and confirms the presence of ChT and T-ChT in the isolated supernatant, thus verifying enzyme displacement from the AuNP. A concentrated mixture of antibody and ChT or T-ChT was electrophoresed in lanes 7 and 8 to yield many non-resolved bands resulting from the proteolytic nature of the enzymes acting on the antibody. Additionally, protein exchange was indirectly confirmed by measuring the antigen-binding activity of the newly formed antibody-AuNP conjugates after displacing ChT and T-ChT from the AuNP surface (Fig. S5). The measured activity of the displaced ChT and T-ChT is presented in Fig. 7. Notably, the displaced T-ChT is highly active. This is in contrast to the displaced ChT which yields reaction rates slightly greater than the negative control. We postulate that the T-ChT adsorbs to the AuNP through an installed thiol and does not require protein unfolding to adsorb. Thus, the structure and activity of T-ChT is conserved after adsorption and displacement from

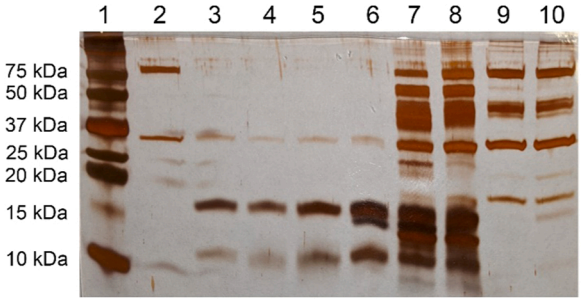

Fig. 8. SDS-PAGE analysis. Lanes from left to right: (1) protein ladder, (2) α-HRP Ab control, (3) ChT control, (4) T-ChT control, (5) ChT concentrated, (6) T-ChT concentrated, (7) ChT + α-HRP Ab concentrated, (8) T-ChT + α-HRP Ab concentrated, (9) ChT conjugate supernatant, (10) T-ChT conjugate supernatant.

the AuNP. However, T-ChT is oriented such that the active site is sterically hindered by the AuNP when adsorbed. In contrast, the ChT must denature to facilitate adsorption and the structure is irreversibly altered to diminish activity after displacement. This is consistent with fluorescence data (Fig. 6) and, collectively, these data suggest that ChT weakly adsorbs to AuNP, denatures, and desorbs.

4. Conclusion

The presence of high affinity functional groups on the surface of a protein is an important factor that dictates the functional fate of a protein adsorbed onto a AuNP. Using an array of complementary analytical methods, we compared the adsorption of ChT, which does not possess a free thiol, and a thiolated ChT analog to AuNPs. The adsorption process was substantially different for the two proteins. Based on a DLS-derived adsorption isotherm, T-ChT possesses a greater adsorption affinity than ChT. Moreover, the thiolated analog resulted in the formation of a hard corona, whereas the native ChT formed a mixed soft/hard protein layer. These two proteins have equivalent molecular weight, charge, and amino acid sequence; thus, we conclude that the installation of surface accessible thiols on T-ChT is responsible for the increased binding affinity. Fluorescence data reveal that the secondary structure of native ChT is altered with prolonged interaction on the AuNP surface. This is consistent with a dynamic ChT layer in which the ChT molecule weakly interacts with the AuNP and undergoes conformational changes, presumably to maximize the binding energy. However, conformational changes are not required to maximize binding interaction for a protein that displays a high affinity thiol group. In a functional assay, neither the ChT-AuNP nor the T-ChT-AuNP bioconjugate is enzymatically active towards a substrate. However, after displacement from the AuNP surface, the T-ChT is biologically active while the ChT is not functional and supports the notion that enzyme orientation is an additional consideration for the performance of a protein-AuNP bioconjugate. Collectively, these data suggest the presence of a solvent accessible thiol on a protein cannot be used as a sole predictor of the loss or gain of protein function when adsorbed on a AuNP but is a useful criterion to anticipate protein denaturation upon adsorption to a AuNP. Additionally, this work establishes that chemical modification of proteins prior to conjugation to AuNPs is a simple and facile approach that can be readily applied to other protein systems for the synthesis of robust and functional conjugates. Future studies will investigate the combined effect of thiolation and other reported parameters that impact enzyme adsorption and structure/activity, including NP curvature, protein size, protein deformability/rigidity, and NP surface charge [17–24].

CRediT authorship contribution statement

M. B. Riley and E. Strandquist were responsible for conducting experiments and analyzing data. C. S. Weitzel assisted in experimental design and data analysis. J. D. Driskell designed experiments, analyzed data, and coordinated the work. All authors contributed to writing the manuscript.

Declaration of Competing Interest

The authors declare that they have no known competing financial interests or personal relationships that could have appeared to influence the work reported in this paper.

Data Availability

Data will be made available on request.

Acknowledgments

This work was funded by the National Science Foundation, USA through the Macromolecular, Supramolecular and Nanochemistry Program, Award # CHE-1807126. Partial support was also provided by Illinois State University. Partial support for E. S. was provided by Illinois State University School of Biological Sciences.

Appendix A. Supporting information

Supplementary data associated with this article can be found in the online version at doi:10.1016/j.colsurfb.2022.112867.

REFERENCES

[1] W. Zhou, X. Gao, D. Liu, X. Chen, Gold Nanoparticles for in Vitro Diagnostics, Chem. Rev. 115 (2015) 10575–10636.
[2] W. Li, X. Chen, Gold Nanoparticles for Photoacoustic Imaging, Nanomedicine 10 (2015) 299–320.
[3] C.J. Murphy, A.M. Gole, J.W. Stone, P.N. Sisco, A.M. Alkilany, E.C. Goldsmith, S. C. Baxter, Gold Nanoparticles in Biology: Beyond Toxicity to Cellular Imaging, Acc. Chem. Res. 41 (2008) 1721–1730.
[4] M.R.K. Ali, Y. Wu, M.A. El-Sayed, Gold-Nanoparticle-Assisted Plasmonic Photothermal Therapy Advances toward Clinical Application, J. Phys. Chem. C. 123 (2019) 15375–15393.
[5] P. Ghosh, G. Han, M. De, C.K. Kim, V.M. Rotello, Gold Nanoparticles in Delivery Applications, Adv. Drug Deliv. Rev. 60 (2008) 1307–1315.
[6] E. Poorakbar, A.A. Saboury, B. Laame Rad, K. Khoshnevisan, Immobilization of Cellulase onto Core-Shell Magnetic Gold Nanoparticles Functionalized by Aspartic Acid and Determination of Its Activity, Protein J. 39 (2020) 328–336.
[7] S.A.R. Kazmi, M.Z. Qureshi, S. Ali, J.-F. Masson, In Vitro Drug Release and Biocatalysis from Ph-Responsive Gold Nanoparticles Synthesized Using Doxycycline, Langmuir 35 (2019) 16266–16274.
[8] J.E. Gagner, M.D. Lopez, J.S. Dordick, R.W. Siegel, Effect of Gold Nanoparticle Morphology on Adsorbed Protein Structure and Function, Biomaterials 32 (2011) 7241–7252.
[9] Z.J. Deng, M.T. Liang, M. Monteiro, I. Toth, R.F. Minchin, Nanoparticle-Induced Unfolding of Fibrinogen Promotes Mac-1 Receptor Activation and Inflammation, Nat. Nanotechnol. 6 (2011) 39–44.
[10] N.O. Fischer, C.M. McIntosh, J.M. Simard, V.M. Rotello, Inhibition of Chymotrypsin through Surface Binding Using Nanoparticle-Based Receptors, P. Natl. Acad. Sci. USA 99 (2002) 5018–5023.
[11] W. Shang, J.H. Nuffer, J.S. Dordick, R.W. Siegel, Unfolding of Ribonuclease a on Silica Nanoparticle Surfaces, Nano Lett. 7 (2007) 1991–1995.
[12] G. Fernandez-Lorente, F. Lopez-Gallego, J.M. Bolivar, J. Rocha-Martin, S. Moreno-Perez, J.M. Guisan, Immobilization of Proteins on Highly Activated Glyoxyl Supports: Dramatic Increase of the Enzyme Stability Via Multipoint Immobilization on Pre-Existing Carriers, Curr. Org. Chem. 19 (2015) 1719–1731.
[13] L. Tarpani, F. Bellezza, P. Sassi, M. Gambucci, A. Cipiciani, L. Latterini, New Insights into the Effects of Surface Functionalization on the Peroxidase Activity of Cytochrome C Adsorbed on Silica Nanoparticles, J. Phys. Chem. B 123 (2019) 2567–2575.
[14] A.M. Abd El-Aziz, M.A. Shaker, M.I. Shaaban, Enhanced Biocatalytic Activity of Recombinant Lipase Immobilized on Gold Nanoparticles, Curr. Pharm. Biotechnol. 20 (2019) 497–505.
[15] F. Gherardi, L. Turyanska, E. Ferrari, N. Weston, M.W. Fay, B.J. Colston, Immobilized Enzymes on Gold Nanoparticles: From Enhanced Stability to Cleaning of Heritage Textiles, ACS Appl. Bio. Mater. 2 (2019) 5136–5143.
[16] P. Asuri, S.S. Karajanagi, H.C. Yang, T.J. Yim, R.S. Kane, J.S. Dordick, Increasing Protein Stability through Control of the Nanoscale Environment, Langmuir 22 (2006) 5833–5836.
[17] K.E. Woods, Y.R. Perera, M.B. Davidson, C.A. Wilks, D.K. Yadav, N.C. Fitzkee, Understanding Protein Structure Deformation on the Surface of Gold Nanoparticles of Varying Size, J. Phys. Chem. C. 120 (2016) 27944–27953.
[18] P. Roach, D. Farrar, C.C. Perry, Surface Tailoring for Controlled Protein Adsorption: Effect of Topography at the Nanometer Scale and Chemistry, J. Am. Chem. Soc. 128 (2006) 3939–3945.
[19] Z.H. Xia, E. Villarreal, H. Wang, B.L.T. Lau, Nanoscale Surface Curvature Modulates Nanoparticle-Protein Interactions, Colloid Surf. B (2020) 190.
[20] S. Tadepalli, Z.Y. Wang, J. Slocik, R.R. Naik, S. Singamaneni, Effect of Size and Curvature on the Enzyme Activity of Bionanoconjugates, Nanoscale 9 (2017) 15666–15672.
[21] G.A. Petkova, K. Zaruba, P. Zvatora, V. Kral, Gold and Silver Nanoparticles for Biomolecule Immobilization and Enzymatic Catalysis, Nanoscale Res. Lett. (2012) 7.
[22] M.E. Aubin-Tam, K. Hamad-Schifferli, Gold Nanoparticle Cytochrome C Complexes: The Effect of Nanoparticle Ligand Charge on Protein Structure, Langmuir 21 (2005) 12080–12084.
[23] S. Tadepalli, Z.Y. Wang, K.K. Liu, Q.S. Jiang, J. Slocik, R.R. Naik, S. Singamaneni, Influence of Surface Charge of the Nanostructures on the Biocatalytic Activity, Langmuir 33 (2017) 6611–6619.
[24] J.M. Dennison, J.M. Zupancic, W. Lin, J.H. Dwyer, C.J. Murphy, Protein Adsorption to Charged Gold Nanospheres as a Function of Protein Deformability, Langmuir 33 (2017) 7751–7761.

[25] S. Dominguez-Medina, et al., Adsorption and Unfolding of a Single Protein Triggers Nanoparticle Aggregation, ACS Nano 10 (2016) 2103–2112.
[26] C. Gunawan, M. Lim, C.P. Marquis, R. Amal, Nanoparticle–Protein Corona Complexes Govern the Biological Fates and Functions of Nanoparticles, J. Mater. Chem. B 2 (2014) 2060–2083.
[27] X. Wu, G. Narsimhan, Characterization of Secondary and Tertiary Conformational Changes of B-Lactoglobulin Adsorbed on Silica Nanoparticle Surfaces, Langmuir 24 (2008) 4989–4998.
[28] J.A. Yang, W. Lin, W.S. Woods, J.M. George, C.J. Murphy, A-Synuclein's Adsorption, Conformation, and Orientation on Cationic Gold Nanoparticle Surfaces Seeds Global Conformation Change, J. Phys. Chem. B 118 (2014) 3559–3571.
[29] A.M. Davidson, M. Brust, D.L. Cooper, M. Volk, Sensitive Analysis of Protein Adsorption to Colloidal Gold by Differential Centrifugal Sedimentation, Anal. Chem. 89 (2017) 6807–6814.
[30] G. Ruiz, K. Tripathi, S. Okyem, J.D. Driskell, Ph Impacts the Orientation of Antibody Adsorbed onto Gold Nanoparticles, Bioconjugate Chem. 30 (2019) 1182–1191.
[31] K. Siriwardana, A. Wang, K. Vangala, N. Fitzkee, D. Zhang, Probing the Effects of Cysteine Residues on Protein Adsorption onto Gold Nanoparticles Using Wild-Type and Mutated Gb3 Proteins, Langmuir 29 (2013) 10990–10996.
[32] K. Vangala, F. Ameer, G. Salomon, V. Le, E. Lewis, L.Y. Yu, D. Liu, D.M. Zhang, Studying Protein and Gold Nanoparticle Interaction Using Organothiols as Molecular Probes, J. Phys. Chem. C. 116 (2012) 3645–3652.
[33] A. Wang, K. Vangala, T. Vo, D. Zhang, N.C. Fitzkee, A. Three-Step, Model for Protein–Gold Nanoparticle Adsorption, J. Phys. Chem. C. 118 (2014) 8134–8142.
[34] F. Liu, L. Wang, H. Wang, L. Yuan, J. Li, J.L. Brash, H. Chen, Modulating the Activity of Protein Conjugated to Gold Nanoparticles by Site-Directed Orientation and Surface Density of Bound Protein, ACS Appl. Mater. Interfaces 7 (2015) 3717–3724.
[35] T. Robson, D.S.H. Shah, A.S. Solovyova, J.H. Lakey, Modular Protein Engineering Approach to the Functionalization of Gold Nanoparticles for Use in Clinical Diagnostics, ACS Appl. Nano Mater. 1 (2018) 3590–3599.
[36] S. Gomez, K. Philippot, V. Collière, B. Chaudret, F. Senocq, P. Lecante, Gold Nanoparticles from Self-Assembled Gold Amine Precursors, Chem. Commun. (2000) 1945–1946.
[37] D.V. Leff, L. Brandt, J.R. Heath, Synthesis and Characterization of Hydrophobic, Organically-Soluble Gold Nanocrystals Functionalized with Primary Amines, Langmuir 12 (1996) 4723–4730.
[38] P.R. Selvakannan, S. Mandal, S. Phadtare, R. Pasricha, M. Sastry, Capping of Gold Nanoparticles by the Amino Acid Lysine Renders Them Water-Dispersible, Langmuir 19 (2003) 3545–3549.
[39] R.C. Rodrigues, C. Ortiz, Á. Berenguer-Murcia, R. Torres, R. Fernández-Lafuente, Modifying Enzyme Activity and Selectivity by Immobilization, Chem. Soc. Rev. 42 (2013) 6290–6307.
[40] F.-L. Gloria, L.-G. Fernando, M.B. Juan, R.-M. Javier, M.-P. Sonia, M.G. Jose, Immobilization of Proteins on Highly Activated Glyoxyl Supports: Dramatic Increase of the Enzyme Stability Via Multipoint Immobilization on Pre-Existing Carriers, Curr. Org. Chem. 19 (2015) 1719–1731.
[41] F. López-Gallego, G. Fernandez-Lorente, J. Rocha-Martin, J.M. Bolivar, C. Mateo, J. M. Guisan, Stabilization of Enzymes by Multipoint Covalent Immobilization on Supports Activated with Glyoxyl Groups, in: J.M. Guisan (Ed.), In Immobilization of Enzymes and Cells: Third Edition, Humana Press, Totowa, NJ, 2013, pp. 59–71.
[42] S. Okyem, O. Awotunde, T. Ogunlusi, M.B. Riley, J.D. Driskell, High-Affinity Points of Interaction on Antibody Allow Synthesis of Stable and Highly Functional Antibody-Gold Nanoparticle Conjugates, Bioconjugate Chem. 32 (2021) 1753–1762.
[43] S. Gault, M.W. Jaworek, R. Winter, C.S. Cockell, High Pressures Increase A-Chymotrypsin Enzyme Activity under Perchlorate Stress, Commun. Biol. 3 (2020) 550.
[44] O. Awotunde, S. Okyem, R. Chikoti, J.D. Driskell, Role of Free Thiol on Protein Adsorption to Gold Nanoparticles, Langmuir 36 (2020) 9241–9249.
[45] G. Ruiz, N. Ryan, K. Rutschke, O. Awotunde, J.D. Driskell, Antibodies Irreversibly Adsorb to Gold Nanoparticles and Resist Displacement by Common Blood Proteins, Langmuir 35 (2019) 10601–10609.
[46] K. Tripathi, J.D. Driskell, Quantifying Bound and Active Antibodies Conjugated to Gold Nanoparticles: A Comprehensive and Robust Approach to Evaluate Immobilization Chemistry, ACS Omega 3 (2018) 8253–8259.
[47] B.C. Mei, E. Oh, K. Susumu, D. Farrell, T.J. Mountziaris, H. Mattoussi, Effects of Ligand Coordination Number and Surface Curvature on the Stability of Gold Nanoparticles in Aqueous Solutions, Langmuir 25 (2009) 10604–10611.
[48] R. Hong, T. Emrick, V.M. Rotello, Monolayer-Controlled Substrate Selectivity Using Noncovalent Enzyme−Nanoparticle Conjugates, J. Am. Chem. Soc. 126 (2004) 13572–13573.
[49] R. Adamczak, A. Porollo, J. Meller, Accurate Prediction of Solvent Accessibility Using Neural Networks–Based Regression, Protein.: Struct., Funct., Bioinforma. 56 (2004) 753–767.
[50] R. Adamczak, A. Porollo, J. Meller, Combining Prediction of Secondary Structure and Solvent Accessibility in Proteins, Protein.: Struct., Funct., Bioinforma. 59 (2005) 467–475.
[51] M. Wagner, R. Adamczak, A. Porollo, J. Meller, Linear Regression Models for Solvent Accessibility Prediction in Proteins, J. Comput. Biol.: a J. Comput. Mol. Cell Biol. 12 (2005) 355–369.
[52] H. Tsukada, D.M. Blow, Structure of Alpha-Chymotrypsin Refined at 1.68 a Resolution, J. Mol. Biol. 184 (1985) 703–711.
[53] E. Jurrus, et al., Improvements to the Apbs Biomolecular Solvation Software Suite, Protein Sci.: a Publ. Protein Soc. 27 (2018) 112–128.
[54] G.L. Ellman, Tissue Sulfhydryl Groups, Arch. Biochem. Biophys. 82 (1959) 70–77.
[55] M. Hirano, D.E. Anderson, H.P. Erickson, T. Hirano, Bimodal Activation of Smc Atpase by Intra- and Inter-Molecular Interactions, EMBO J. 20 (2001) 3238–3250.
[56] M. Hirano, T. Hirano, Hinge-Mediated Dimerization of Smc Protein Is Essential for Its Dynamic Interaction with DNA, EMBO J. 21 (2002) 5733–5744.
[57] Y. Li, C.S. Weitzel, R.J. Arnold, M.G. Oakley, Identification of Interacting Regions within the Coiled Coil of the Escherichia coli Structural Maintenance of Chromosomes Protein Mukb, J. Mole. Biol. 391 (2009) 57–73.
[58] C.S. Weitzel, V.M. Waldman, T.A. Graham, M.G. Oakley, A Repeated Coiled-Coil Interruption in the Escherichia coli Condensin Mukb, J. Mol. Biol. 414 (2011) 578–595.
[59] V.M. Waldman, T.H. Stanage, A. Mims, I.S. Norden, M.G. Oakley, Structural Mapping of the Coiled-Coil Domain of a Bacterial Condensin and Comparative Analyses across All Domains of Life Suggest Conserved Features of Smc, Proteins Proteins 83 (2015) 1027–1045.
[60] D. Baimanov, R. Cai, C.Y. Chen, Understanding the Chemical Nature of Nanoparticle-Protein Interactions, Bioconjugate Chem. 30 (2019) 1923–1937.
[61] K. Giri, et al., Understanding Protein-Nanoparticle Interaction: A New Gateway to Disease Therapeutics, Bioconjugate Chem. 25 (2014) 1078–1090.
[62] O. Vilanova, J.J. Mittag, P.M. Kelly, S. Milani, K.A. Dawson, J.O. Radler, G. Franzese, Understanding the Kinetics of Protein-Nanoparticle Corona Formation, ACS Nano 10 (2016) 10842–10850.
[63] I. Yadav, S. Kumar, V.K. Aswal, J. Kohlbrecher, Structure and Interaction in the Ph-Dependent Phase Behavior of Nanoparticle-Protein Systems, Langmuir 33 (2017) 1227–1238.
[64] N.G. Khlebtsov, V.A. Bogatyrev, L.A. Dykman, A.G. Melnikov, Spectral Extinction of Colloidal Gold and Its Biospecific Conjugates, J. Colloid Interf. Sci. 180 (1996) 436–445.
[65] M.J. Pollitt, G. Buckton, R. Piper, S. Brocchini, Measuring Antibody Coatings on Gold Nanoparticles by Optical Spectroscopy, RSC Adv. 5 (2015) 24521–24527.
[66] E.J.W. Verwey, J.T.G. Overbeek, Theory of the Stability of Lyophobic Colloids: The Interaction of Sol Particles Having an Electric Double Layer, Elsevier,, Amsterdam, 1948, p. 205.
[67] L.A. Wijenayaka, M.R. Ivanov, C.M. Cheatum, A.J. Haes, Improved Parametrization for Extended Derjaguin, Landau, Verwey, and Overbeek Predictions of Functionalized Gold Nanosphere Stability, J. Phys. Chem. C. 119 (2015) 10064–10075.
[68] R. Kozlowski, A. Ragupathi, R.B. Dyer, Characterizing the Surface Coverage of Protein–Gold Nanoparticle Bioconjugates, Bioconjugate Chem. 29 (2018) 2691–2700.
[69] A.B. Ghisaidoobe, S.J. Chung, Intrinsic Tryptophan Fluorescence in the Detection and Analysis of Proteins: A Focus on Förster Resonance Energy Transfer Techniques, Int. J. Mol. Sci. 15 (2014) 22518–22538.
[70] M. Kessenbrock, G. Groth, in: B.M. Binder, G. Eric Schaller (Eds.), Circular Dichroism and Fluorescence Spectroscopy to Study Protein Structure and Protein–Protein Interactions in Ethylene Signaling. In Ethylene Signaling: Methods and Protocols, Springer, New York: New York, NY, 2017, pp. 141–159.